

Chemical dynamics of cyclopropynylidyne ($c\text{-C}_3\text{H}; X^2B_2$) formation from the reaction of $C(^1D)$ with acetylene, $C_2H_2(X^1\Sigma_g^+)$

R. I. Kaiser,^{a)} A. M. Mebel, and Y. T. Lee

Institute of Atomic and Molecular Sciences, 1, Section 4, Roosevelt Rd., 107 Taipei, Taiwan, Republic of China

(Received 28 July 2000; accepted 13 October 2000)

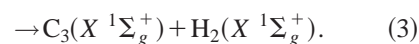
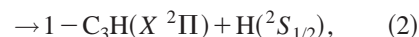
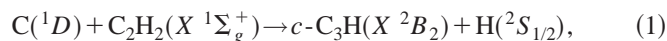
The reaction between electronically excited carbon atoms, $C(^1D)$, and acetylene was studied at two average collision energies of 45 kJ mol^{-1} and 109 kJ mol^{-1} employing the crossed molecular beam technique. The time-of-flight spectra recorded at mass to charge $m/e=37(C_3H^+)$ and $m/e=36(C_3^+)$ show identical patterns indicating the existence of a carbon versus atomic hydrogen exchange pathway to form C_3H isomer(s); no H_2 elimination to the thermodynamically favorable tricarbon channel was observed. Forward-convolution fitting of our data shows that the reaction proceeds via direct stripping dynamics on the $^1A'$ surface via an addition of the carbon atom to the π -orbital of acetylene to form a highly rovibrationally, short lived cyclopropenylidene intermediate which decomposes by atomic hydrogen emission to $c\text{-C}_3\text{H}(X^2B_2)$. The dynamics of this reaction have important impact on modeling of chemical processes in atmospheres of comets approaching the perihelion as photolytically generated $C(^1D)$ atoms are present. © 2001 American Institute of Physics. [DOI: 10.1063/1.1330232]

I. INTRODUCTION

The reactions of electronically excited first row atoms $C(^1D)$, $N(^2D)$, and $O(^1D)$ are of fundamental importance in chemical reaction dynamics, and of paramount impact in combustion processes, atmospheric chemistry of Earth, and hydrocarbon rich planets in the outer solar system, as well as the coma of comets approaching our sun. Whereas a multitude of kinetic data as well as crossed molecular beam studies have been reported on the ground state $C(^3P)$, $N(^4S)$, and $O(^3P)$ beams,¹ the chemical reaction dynamics of the excited counterparts are sparse. This is mainly due to the experimental difficulty to prepare a stable and high intensity beam of electronically excited atoms to guarantee a detectable quantity of final products and a reasonable signal-to-noise ratio. Crossed beam studies of $O(^1D)$ with $H_2(D_2)$,² halogenated hydrocarbons such as CF_3Br ,³ hydrogenhalides HCl ,⁴ HBr ,⁵ HI ,⁶ and hydrogen sulfide⁷ have been studied, just to name a few. A high intensity continuous $N(^2D)$ source was developed by Casavecchia and co-workers and employed in crossed beam experiments with acetylene,⁸ ethylene,⁹ and D_2 .¹⁰

An investigation of $C(^1D)$ reactions on the most fundamental, microscopic level have been very meager. Reisler and co-workers studied the $C(^1D)/H_2$ and $C(^1D)/HCl$ systems employing laser induced fluorescence detection.¹¹ Very recently, Casavecchia *et al.* performed a crossed molecular beam experiment of a continuous $C(^1D)$ beam with H_2 . This reaction proceeds solely via an insertion of $C(^1D)$ into the H–H bond to form atomic hydrogen plus the methylidene radical, $CH(^2\Pi_g)$.¹² Whereas this system may be regarded as

a prototype for $C(^1D)$ reactions because of its simplicity, the reaction mechanism with unsaturated hydrocarbons is expected to be different, with the addition of electronically excited carbon to the π system being dominant. Although electronically excited atoms play no role in the chemistry in the interstellar medium due to their life time in the order of hours, elementary reactions of $C(^1D)$ in comets are of fundamental importance as their production rate coma of Halley at distances of 50 000 km from the sun is calculated to $2.4 \times 10^{27} \text{ s}^{-1}$. The main source is photoionization of carbon monoxide, CO, followed by subsequent dissociative recombination of CO^+ ions with electrons.¹³ In the present paper, we investigate the first crossed beam study of electronically excited carbon atoms with the polyatomic unsaturated molecules, i.e., acetylene, on the most fundamental level to form C_3H isomers and atomic hydrogen and/or tricarbon plus molecular hydrogen, cf. reactions (1)–(3). These investigations are supplemented by electronic structure calculations on the C_3H_2 and C_3H potential energy surfaces:



II. EXPERIMENTAL SETUP

Reactive scattering experiments are conducted in a universal crossed molecular beam apparatus.¹⁴ Briefly, the 30 Hz, 35–40 mJ output of a Nd:YAG laser is focused onto a rotating carbon rod. Ablated carbon atoms are seeded into helium released by a pulsed valve operating at 60 Hz. A four-slot chopper wheel selects a $9.0 \mu\text{s}$ segment of the fast part of the carbon beam with velocities of $3196 \pm 106 \text{ ms}^{-1}$ and $5079 \pm 230 \text{ ms}^{-1}$ and speed ratios of 2.6 and 2.0, respectively. Selecting a part of the pulse in the velocity regime

^{a)}Also at: Department of Physics, University Chemnitz, 09107 Chemnitz, Germany. Corresponding author. Electronic mail: kaiser@po.iams.sinica.edu.tw

between 3000 and 4000 ms^{-1} generates $\text{C}(^3P_j/{}^1D)$; even faster parts of the beam contain almost exclusively $\text{C}({}^1D)$. This pulsed carbon beam crosses a second continuous acetylene beam of a velocity 866 ms^{-1} at 90° in the interaction region of the scattering chamber at relative collision energies E_C of $45.0 \pm 3.0 \text{ kJ mol}^{-1}$ and $109 \pm 10 \text{ kJ mol}^{-1}$. Reactively scattered products were detected in the plane defined by both beams using a rotatable detector with a Brink-type electron-impact ionizer, quadrupole mass filter, and a Daly ion detector at distinct laboratory angles. Velocity distributions of the products were recorded using the time-of-flight (TOF) technique. A forward-convolution routine is used to fit the TOF spectra and the product angular distribution in the laboratory frame (LAB distribution). This procedure initially assumes the angular flux distribution $T(\theta)$ and the translational energy flux distribution $P(E_T)$ in the center-of-mass system (CM). TOF spectra and LAB distribution are then calculated from $T(\theta)$ and $P(E_T)$ and refined until a reasonable fit is achieved. The ultimate outcome is the generation of a velocity flux contour map $I(\theta, u)$ showing the intensity I as a function of center-of-mass angle θ and velocity u in the CM frame.

III. ELECTRONIC STRUCTURE CALCULATIONS

Geometries of the reactants, products, various intermediates, and transition states for the title reaction were optimized using the hybrid density functional B3LYP method, i.e., Becke's three-parameter nonlocal exchange functional¹⁴ with the nonlocal correlation functional of Lee, Yang, and Parr,¹⁵ and the 6-311G(*d,p*) basis set.¹⁶ Vibrational frequencies, calculated at the B3LYP/6-311G(*d,p*) level, were used for characterization of stationary points and zero-point energy (ZPE) correction. All stationary points were positively identified for minimum or transition state. In some cases, geometries and frequencies were recalculated at the MP2/6-311G(*d,p*) and CCSD(T)/6-311G(*d,p*) levels.¹⁷ The GAUSSIAN 94,¹⁸ MOLPRO 96,¹⁹ and ACES-II²⁰ programs were employed for the potential energy surface computations. The accuracy of our calculations is about $\pm 5 \text{ kJ mol}^{-1}$.

IV. RESULTS

A. Reactive scattering signal

Reactive scattering signal was detected at mass to charges $m/e=37(\text{C}_3\text{H}^+)$ (Figs. 1 and 2) and $m/e=36(\text{C}_3^+)$. TOF spectra at $m/e=36$ show identical patterns indicating that this signal originates in cracking of the parent in the ionizer and that the spin allowed channel 3 to form tricarbon and molecular hydrogen is absent within our detection limits. Further, no radiative association to C_3H_2 ($m/e=38$) could be observed.

B. Lab distribution and TOF spectra

Figures 3 and 4 show the most probable Newton diagrams of the reaction $\text{C}({}^1D) + \text{C}_2\text{H}_2(X^1\Sigma_g^+)$ together with the LAB distributions of the C_3H product(s). The circles stand for the maximum center-of-mass recoil velocity of the $c\text{-C}_3\text{H}$ product assuming all available energy channels into

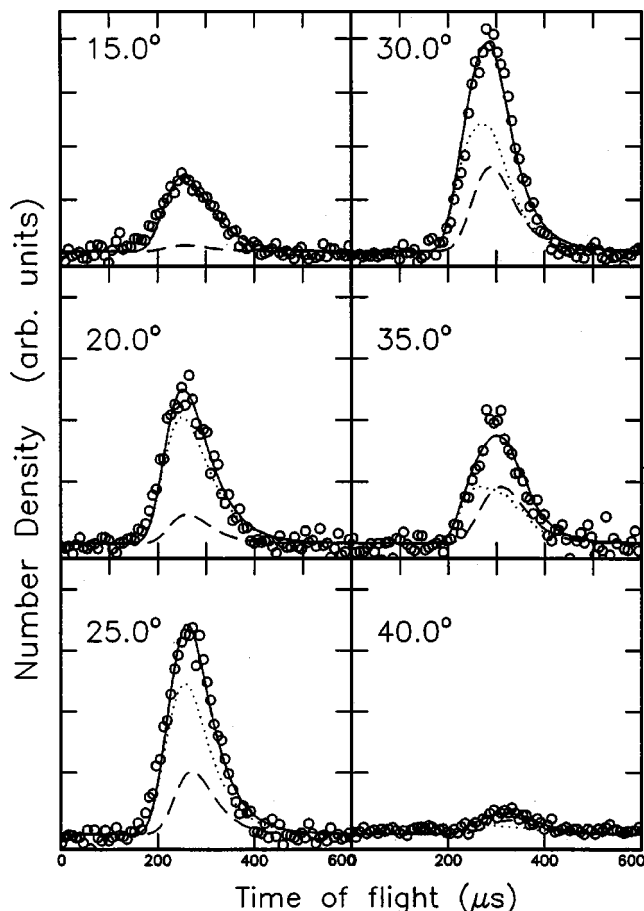


FIG. 1. Time-of-flight data for the reaction $\text{C}(^3P_j)/\text{C}({}^1D) + \text{C}_2\text{H}_2(X^1\Sigma_g^+)$ at $m/e=37$ recorded at a collision energy of 45 kJ mol^{-1} for indicated laboratory angles. Open circles represent experimental data, dashed, and dotted lines the calculated distributions for $\text{C}(^3P_j)$ and $\text{C}({}^1D)$, and the solid line the sum of the fit.

the translational degrees of freedom. The calculations were performed for the $\text{C}({}^1D) + \text{C}_2\text{H}_2(X^1\Sigma_g^+) \rightarrow c\text{-C}_3\text{H}(X^2B_2) + \text{H}({}^2S_{1/2})$ reaction (outer circles) and compared to the reaction of ground state carbon atoms, $\text{C}(^3P_j) + \text{C}_2\text{H}_2(X^1\Sigma_g^+) \rightarrow c\text{-C}_3\text{H}(X^2B_2) + \text{H}({}^2S_{1/2})$. At lower collision energy, the experimental data must be fit with two channels arising from reactions of ground state carbon (dashed lines) and electronically excited carbon (dotted lines), cf. Figs. 3 and 4. As the collision energy rises, a reasonable fit could be achieved with a primary beam consisting solely of $\text{C}({}^1D)$. The reaction dynamics of ground state carbon atoms with acetylene were discussed extensively in Ref. 21, and hence we restrict ourselves to the channel arising from electronically excited carbon. At both collision energies, the LAB distributions are forward scattered with respect to the CM angles at 30.4° and 20.3° and peak at about 27° and 15° , respectively. As the collision energy rises, the forward scattering is more pronounced. These data suggest that the reaction proceeds either via indirect scattering dynamics through an osculating complex or via a direct reaction mechanism. Further, both LAB distributions are very broad and spread about 40° – 50° in the scattering plane defined by both beams. This finding proposes a large energy release into translational degrees of freedom of the C_3H and H products as well as a center-of-

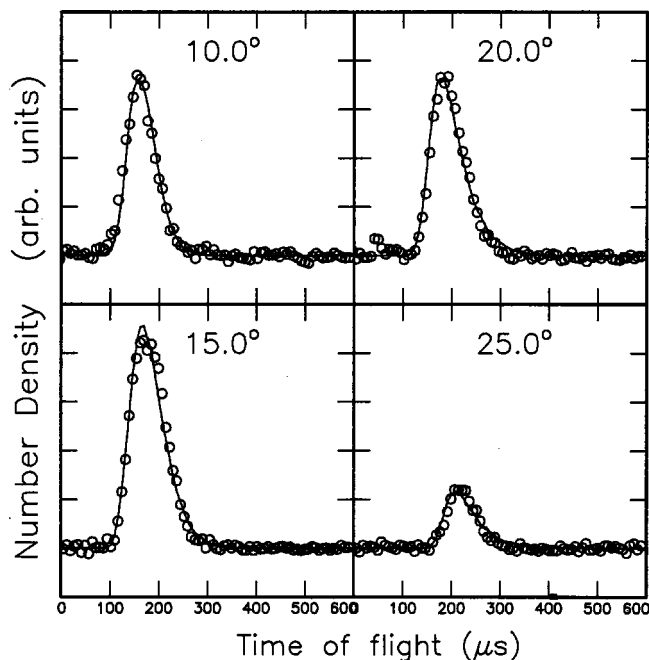


FIG. 2. Time-of-flight data for the reaction $C(^1D) + C_2H_2(X^1\Sigma_g^+)$ at $m/e = 37$ recorded at a collision energy of 109 kJ mol^{-1} for indicated laboratory angles. Open circles represent experimental data, the solid line the fit.

mass translational energy distribution peaking away from zero. Further, the scattering ranges correlate nicely with the presence of electronically excited carbon atoms in the primary beam: here, we expect cutoffs at 5° and 55° ($E_C = 45.0 \pm 3.0 \text{ kJ mol}^{-1}$) and -5° and 30° ($E_C = 109 \pm 10 \text{ kJ mol}^{-1}$); these data are in close agreement with our experimental results.

C. Center-of-mass translational energy distributions, $P(E_T)$

The center-of-mass translational energy distributions $P(E_T)$ are presented in Figs. 5 and 6 together with the center-of-mass angular distributions $T(\theta)$. Best fits of TOF spectra and LAB distributions were achieved with $P(E_T)$'s extending to the maximum translational energy E_{\max} = $190\text{--}220 \text{ kJ mol}^{-1}$ and $250\text{--}290 \text{ kJ mol}^{-1}$ at lower and higher collision energy, respectively. Extending or cutting the fits by $20\text{--}30 \text{ kJ mol}^{-1}$ does not change the fit dramatically. Both E_{\max} limits can be analyzed to assign the reaction product if their energetics are well separated; further, our experimental reaction energies can be compared with the electronic structure calculations. Since the maximum available energy is simply the sum of the reaction exothermicity plus the collision energy, we can subtract the latter from E_{\max} and yield experimental exothermicities of $145\text{--}175 \text{ kJ mol}^{-1}$ and $141\text{--}181 \text{ kJ mol}^{-1}$ at $E_C = 45.0 \pm 3.0 \text{ kJ mol}^{-1}$ and $E_C = 109 \pm 10 \text{ kJ mol}^{-1}$. This is in very close agreement to our *ab initio* data predicting exothermicities of 142.3 and $150.6 \text{ kJ mol}^{-1}$ to form *l*- C_3H and *c*- C_3H , respectively, from reaction of $C(^1D)$ with acetylene. This is an unambiguous proof that our primary beam contains carbon in its first electronically excited $C(^1D)$ state: the reactions with ground state carbon, $C(^3P_j)$ is about 141 kJ mol^{-1}

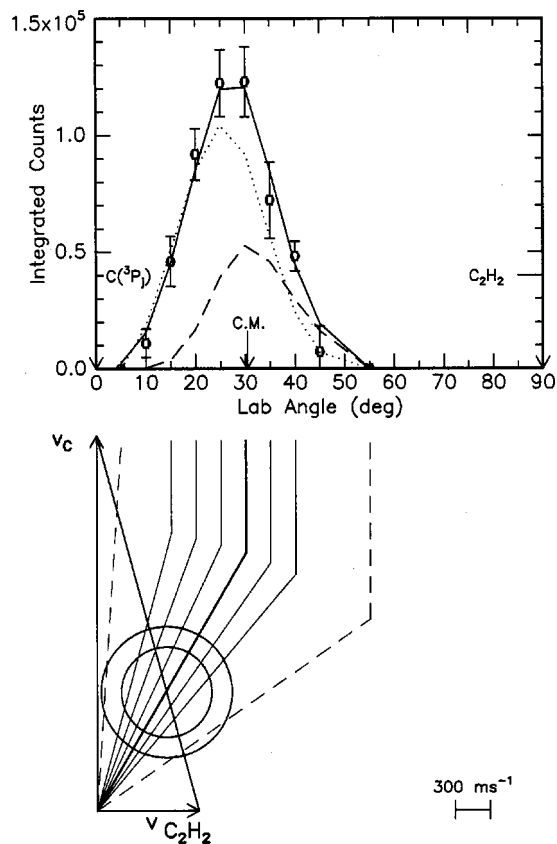


FIG. 3. Lower: Newton diagram for the reaction $C(^3P_j)/C(^1D) + C_2H_2(X^1\Sigma_g^+)$ at a collision energy of 45 kJ mol^{-1} . Upper: Laboratory angular distribution of C_3H product channel at $m/e = 37$. Circles and 1σ error bars indicate experimental data, the dashed and dotted lines the calculated distributions for $C(^3P_j)$ and $C(^1D)$, and the solid line the sum. C.M. designates the center-of-mass angle. The solid lines originating in the Newton diagram point to distinct laboratory angles whose TOFs are shown in Fig. 1.

less exothermic. However, since the energetics of the linear and cyclic C_3H are separated by only 8 kJ mol^{-1} , we cannot identify the isomer at the present point and hence must investigate the involved chemical reaction dynamics to assign the reaction product(s), cf. Sec. V. Further, the $P(E_T)$'s peak far away from zero translational energy at about 60 kJ mol^{-1} and 120 kJ mol^{-1} at lower and higher collision energy, respectively. Together with the averaged fraction of energy released into translational motion of the products, i.e., $50\%\text{--}55\%$ and ca. 60% at lower and higher collision energy, the reaction proceeds very likely via direct scattering dynamics.

D. Center-of-mass angular distributions, $T(\theta)$, and flux contour maps, $I(u, \theta)$

As expected from the LAB distributions, both center-of-mass angular distributions (Figs. 5 and 6) and contour maps (Figs. 7 and 8) predominantly show flux in the forward hemisphere with respect to the carbon beam. Both distributions peak at 0° , and show no intensity at angles larger than 100° and $46^\circ\text{--}50^\circ$, at lower and higher collision energies, respectively. Hence the initial and final angular momenta \mathbf{L} and \mathbf{L}' are strongly correlated. These findings verify our assumption that the reaction proceeds via direct reaction dynamics

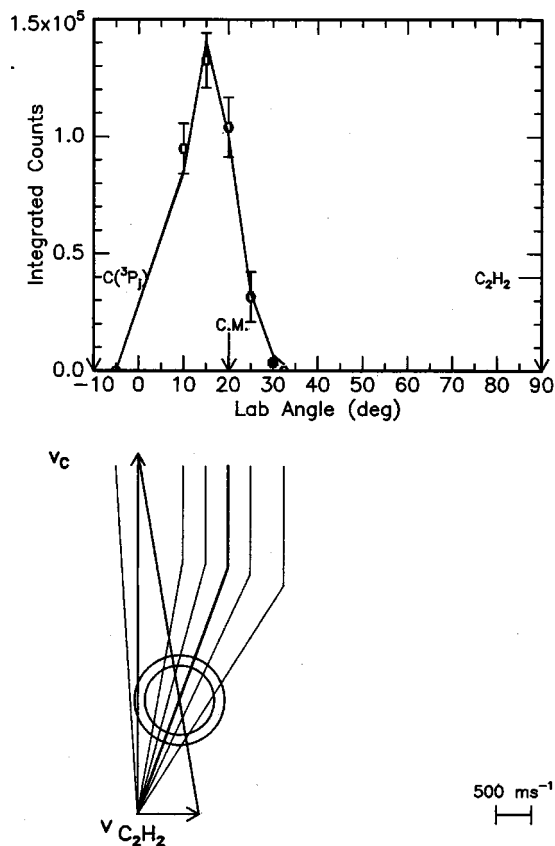


FIG. 4. Lower: Newton diagram for the reaction $C(^1D) + C_2H_2(X^1\Sigma_g^+)$ at a collision energy of 109 kJ mol^{-1} . Upper: Laboratory angular distribution of C_3H product channel at $m/e=37$. Circles and 1σ error bars indicate experimental data, the solid line the calculated distribution. C.M. designates the center-of-mass angle. The solid lines originating in the Newton diagram point to distinct laboratory angles whose TOFs are shown in Fig. 2.

(stripping mechanism) within a time scale of less than 0.1–0.2 ps. In the following sections we have to discriminate if the potential energy surface (PES) involves a highly rovibrationally (or even electronically) excited C_3H_2 collision complex in a very shallow potential energy well, or only a transition state $[C_3H_2]^*$ along the reaction coordinate without a bound intermediate.

V. DISCUSSION

A. The singlet C_3H_2 *ab initio* potential energy surface

Cyclopropenylidene *c*- C_3H_2 in its 1A_1 electronic ground state is the global minimum of the C_3H_2 potential energy surface (PES); Figs. 9 and 10. It belongs to the C_{2v} point group and is stabilized by $572.4 \text{ kJ mol}^{-1}$ with respect to the separated reactants. The stability of this isomer can be associated with the aromatic character of its X^1A_1 state characterizing cyclopropenylidene as a 2π Hückel system.²² All atoms are in one plane; the carbon–carbon distances slightly alternate between 1.323 \AA (olefinic) and 1.423 \AA (aliphatic to olefinic), whereas the carbon–hydrogen length is 1.080 \AA close to an aromatic system. The singlet–triplet splitting between the ground state cyclopropenylidene and the lowest triplet state of this isomer is calculated to be about 225

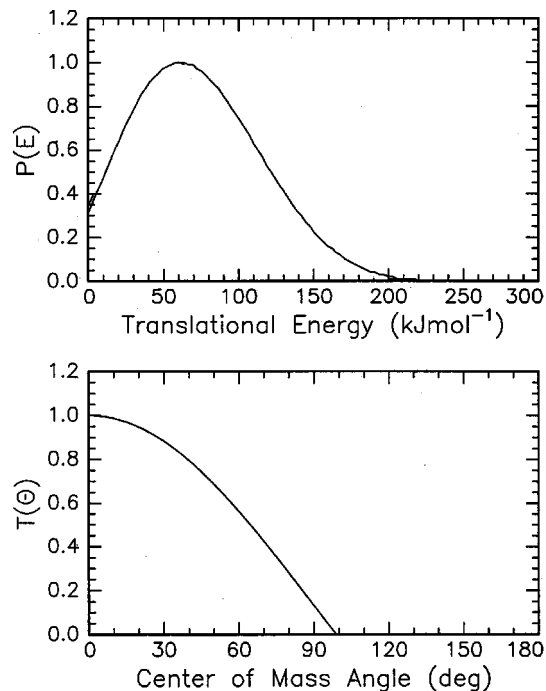


FIG. 5. Center-of-mass angular flux distribution (lower) and translational energy flux distribution (upper) for the reaction $C(^1D) + C_2H_2(X^1\Sigma_g^+) \rightarrow C_3H + H(^2S_{1/2})$ at a collision energy of 45 kJ mol^{-1} .

kJ mol^{-1} .²³ Note that experimental data of $\Delta H_f(293 \text{ K})$ were determined via photoelectron spectroscopy to $478 \pm 17 \text{ kJ mol}^{-1}$.²⁴

The second isomer, vinylidene H_2CCC , has C_{2v} symmetry in its 1A_1 ground state. The enthalpy of formation of this structure is calculated to be $\Delta H_f(0 \text{ K})$

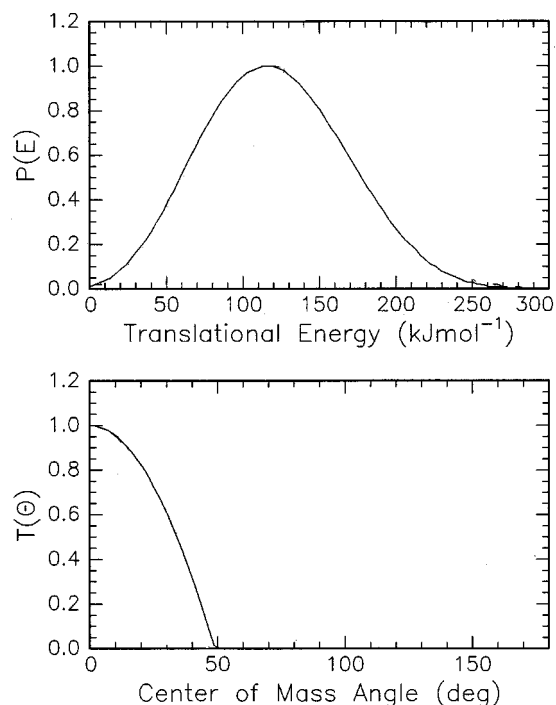


FIG. 6. Center-of-mass angular flux distribution (lower) and translational energy flux distribution (upper) for the reaction $C(^1D) + C_2H_2(X^1\Sigma_g^+) \rightarrow C_3H + H(^2S_{1/2})$ at a collision energy of 109 kJ mol^{-1} .

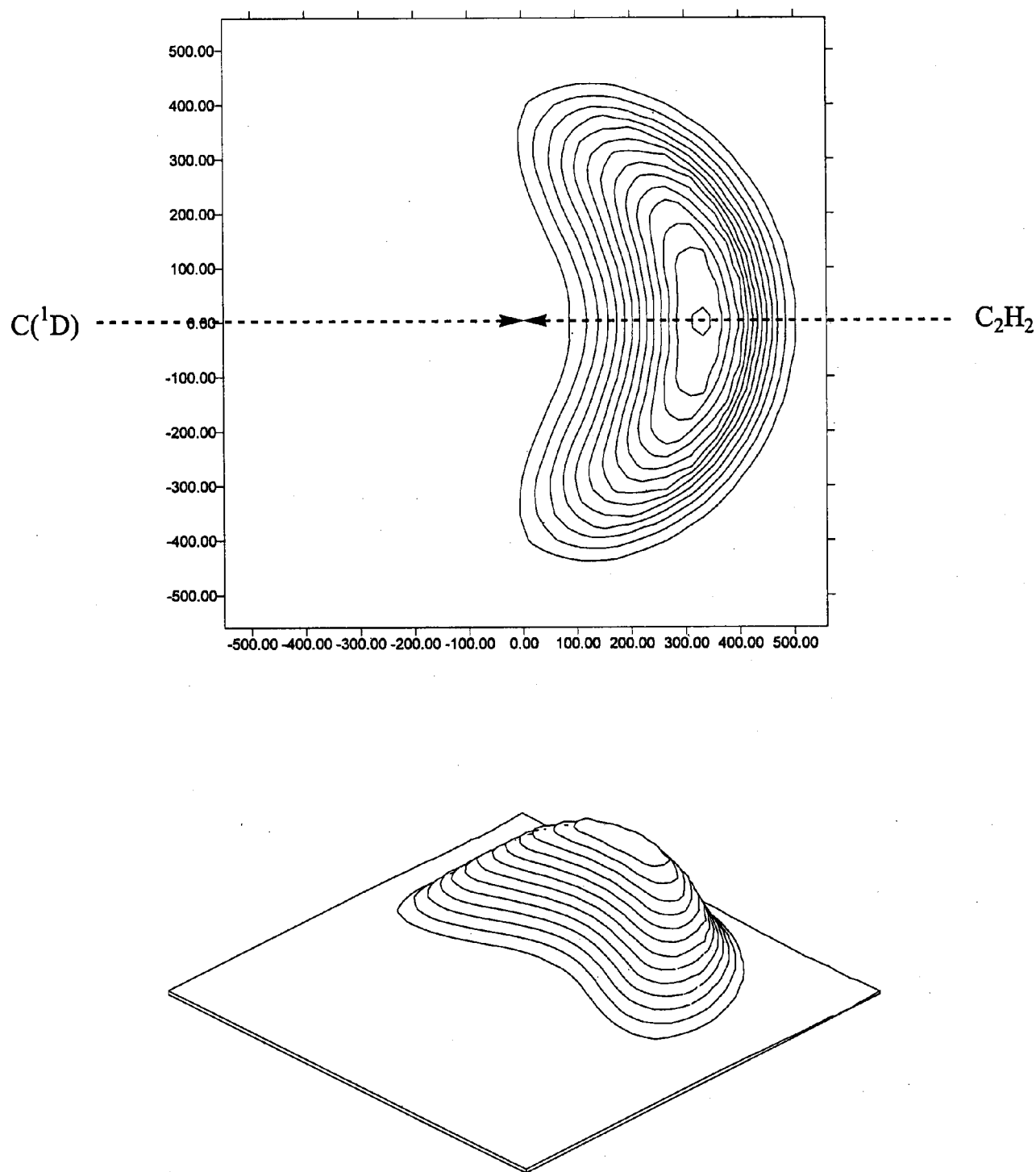


FIG. 7. Contour flux map for the reaction $C(^1D) + C_2H_2(X\ ^1\Sigma_g^+) \rightarrow C_3H + H(^2S_{1/2})$ at a collision energy of 45 kJ mol^{-1} . Top: two-dimensional projection, bottom: three-dimensional map. Units are given in ms^{-1} .

$= 441.7\text{ kJ mol}^{-1}$ thus being 56.5 kJ mol^{-1} less stable than the cyclopropenylidene isomer. These data are in good agreement with older calculations depicting a destabilization of $41.9\text{--}62.9\text{ kJ mol}^{-1}$.²⁵ Its carbenic structure is well reflected by its internal coordinates; the carbon-carbon bonds are 1.332 \AA (olefinic) and 1.285 \AA (olefinic to acetylenic), whereas the C–H–H and H–C–H angles are 121.7° and 116.6° , suggesting an almost sp^2 hybridization of this carbon atom. These data correlate nicely with the equilibrium geom-

etry extracted from rotational spectra, i.e., 121.2° and 117.6° , respectively, as well carbon-carbon distances of 1.328 \AA and 1.291 \AA .²⁶ Finally, the singlet-triplet splitting between the $X\ ^1A_1$ and $a\ ^3B_1$ states is 246 kJ mol^{-1} based on our data and Ref. 25.

The third isomer, propargylene, is the energetically least stable singlet C_3H_2 species. This molecule has C_s symmetry, a $^1A'$ electronic wave function, and is less stable by about 100 kJ mol^{-1} with respect to cyclopropenylidene. Its en-

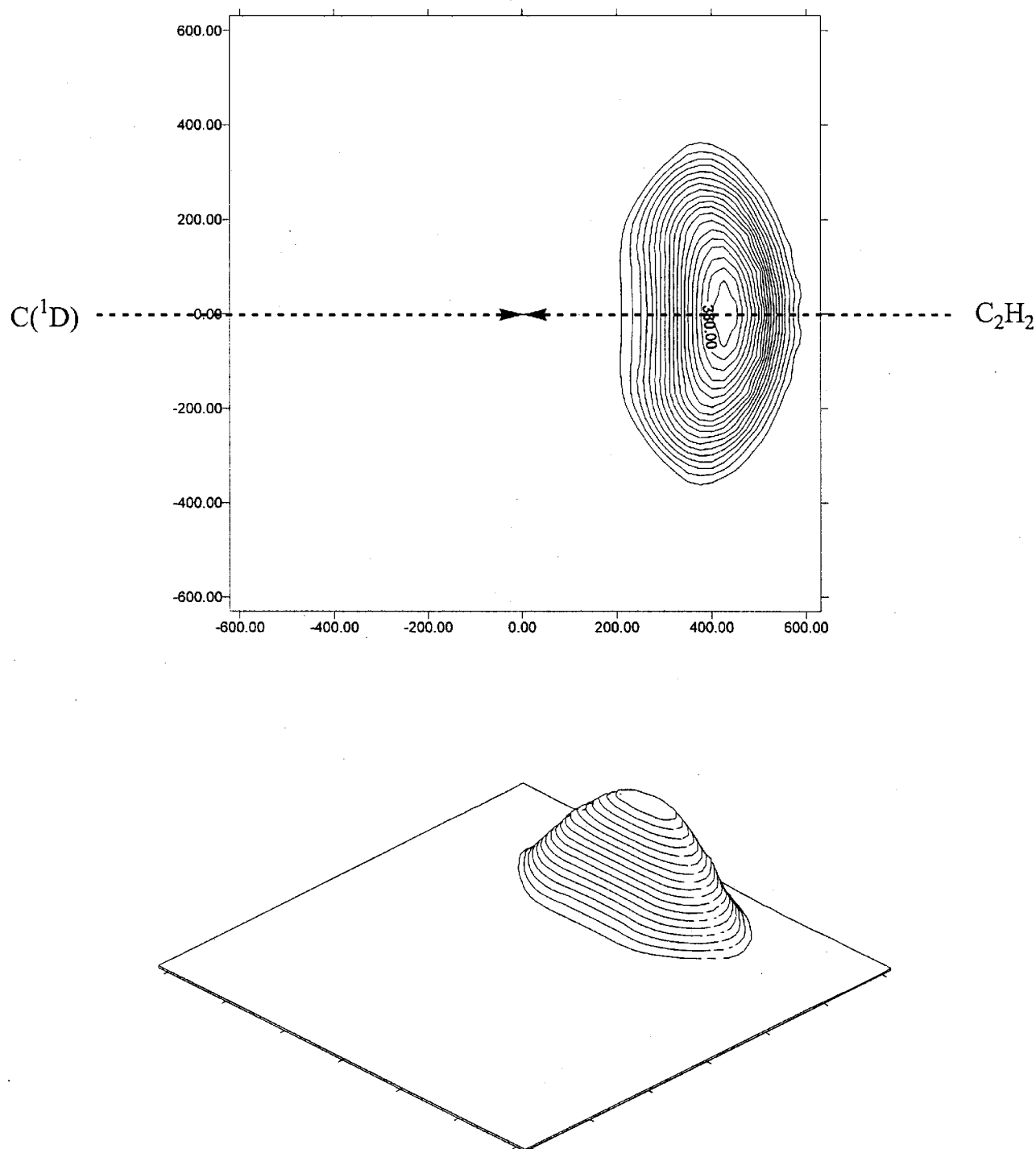


FIG. 8. Contour flux map for the reaction $C(^1D) + C_2H_2(X^1\Sigma_g^+) \rightarrow C_3H + H(^2S_{1/2})$ at a collision energy of 109 kJ mol^{-1} . Top: two-dimensional projection, bottom: three-dimensional map. Units are given in ms^{-1} .

thalpy of formation is calculated to be about $\Delta H_f(0 \text{ K}) = 598.2 \text{ kJ mol}^{-1}$, about 45 kJ mol^{-1} higher than its $^3A''$ triplet state.²⁷ The equilibrium geometry depicts an almost linear carbon skeleton with a carbon chain deviating $14^\circ - 7^\circ$ from linearity, and the carbon-carbon distances are 1.244 \AA (almost acetylenic bond) and 1.374 \AA (almost pure olefinic bond). Compared to the triplet C_3H_2 PES, singlet cis/trans propenediylidene structures were found to collapse to cyclopropenylidene upon optimization; this finding is in strong

agreement with Takahashi *et al.*²⁸ Further, a hypothetical singlet cyclopropyne is found to be a transition state to vinylidenecarbene. This correlates with previous studies of Sherrill *et al.* and Mebel *et al.*²⁹ All singlet C_3H_2 isomers are connected via various transition states which are well below the total energy of the separated reactants. Cyclopropenylidene can be formed via an initial addition of the electronically excited carbon atom to the carbon-carbon triple bond of the acetylene molecule without entrance barrier. It

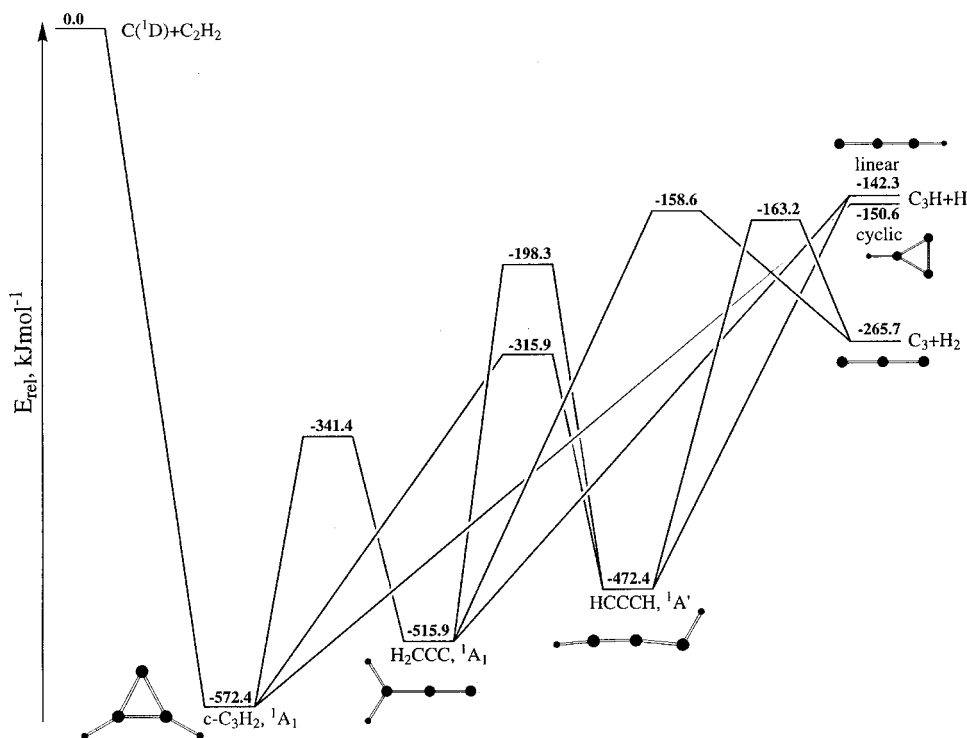


FIG. 9. Schematic representation of the singlet C_3H_2 potential energy surface.

can isomerize either to vinylidenecarbene via hydrogen migration/ring opening or to propargylene through ring opening or decays barrier less to atomic hydrogen and $c-C_3H(X^2B_2)$. Vinylidenecarbene shows three feasible reaction pathways as a hydrogen migration connects to propargylene, a barrier less atomic hydrogen loss to the liner tricarbon hydride, $C_3H(X^2\Pi)$, and a molecular hydrogen elimination to tricarbon, $C_3(X^1\Sigma_g^+)$. Finally, propargylene can fragment via atomic or molecular hydrogen elimination to linear tricarbon hydride or tricarbon, respectively. We like to stress that we were unable to find a transition state of an initial insertion of $C(^1D)$ into the carbon–hydrogen bond of acetylene to form propargylene. Likewise, we could not locate a transition state from the reactants to any C_3H isomer.

B. The reaction pathway

Our theoretical and experimental data were combined to give a coherent picture of the involved chemical dynamics on the reaction of $C(^1D)$ with acetylene. First, the explicit identification of the carbon versus atomic hydrogen exchange proves the formation of a C_3H isomer. This conclusion is verified by comparing our *ab initio* reaction energies (-142.3 and -150.6 kJ mol^{-1} to the linear and cyclic isomer, respectively) with the experimental data of 141 – 181 kJ mol^{-1} . The energetically more favorable reaction to form tricarbon and molecular hydrogen (C_3+H_2) is not observed experimentally although the thermodynamics and spin conservation allow this pathway. Our findings propose an initial addition of atomic carbon to the carbon–carbon triple bond of the acetylene molecule to form the cyclopropynylidyne isomer. This pathway can follow either C_s or C_{2v} symmetry [perpendicular approach of $C(^1D)$ to the carbon–carbon bond]. Based on the PES, this C_3H_2 isomer resides in a deep potential energy well of 572.4 kJ mol^{-1} and 231.0 kJ mol^{-1}

with respect to the reactants and the transition state connecting cyclopropynylidyne to vinylidenecarbene. Therefore, a long lived or at least an osculating complex and indirect scattering dynamics which in turn should be reflected in a forward–backward symmetric or slightly forward scattered center-of-mass angular distribution $T(\theta)$ are anticipated. However, the experimental findings clearly demonstrate a clearly forward scattered C_3H product: a typical stripping mode behavior in the spectator limit which is dominated by an attractive interaction of both reactants and large impact

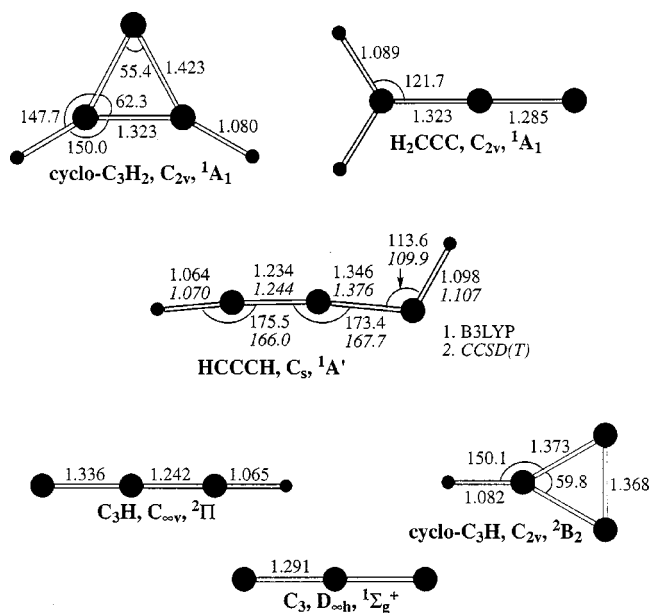


FIG. 10. Structures of potentially involved singlet C_3H_2 collision complexes and possible products. Bond lengths are given in Angstrom, bond angles in degrees.

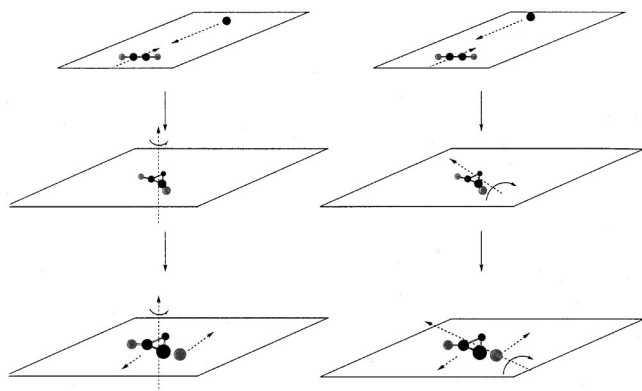


FIG. 11. Schematic representation of the $C(^1D) + C_2H_2(X^1\Sigma_g^+) \rightarrow c\text{-}C_3H + H(^2S_{1/2})$ reaction together with the rotational excitation of the $c\text{-}C_3H$ product.

parameters leading to the reaction. Hence the $C(^1D)$ simply ‘‘picks up’’ the C_2H unit of the acetylene molecule and carries it in the ‘‘forward’’ direction. This is well documented in our strong correlation of the initial and final angular momentum L and L' as found experimentally. Further, based on momentum conservation, the H atom must recoil in the opposite, ‘‘backward’’ direction. Figure 11 shows a cartoon of two reaction pathways leading to rotationally excited $c\text{-}C_3H$ rotating around the B (left side) and C axis (right side). This reaction happens in a time scale of typically 0.1–0.2 ps. Therefore, we must conclude that the lifetime of the initially formed C_3H_2 complex is very short and that this intermediate is very likely formed highly rovibrationally excited. These data translate into an incomplete energy randomization in the cyclopropenylidene adduct; further, a large fraction of available energy channeling into translational energy of the products is expected as verified experimentally to 50%–60%. Our interpretation gains full support from the nondetection of the H_2 elimination channel to form tricarbon. The time scale of this reaction is too short for a hydrogen migration from cyclopropenylidene to either vinylidenecarbene or propargylene. Both latter isomers however are the sole structures which can lead via H_2 elimination to tricarbon, cf. Fig. 10; no transition state was found connecting cyclopropenylidene to $C_3 + H_2$. Therefore, we can conclude that neither vinylidenecarbene nor propargylene are involved in the chemical dynamics of the title reaction under our experimental conditions and that a very short lived rovibrationally cyclopropenylidene is the decomposing intermediate which fragments via H atom emission to the $c\text{-}C_3H$ isomer. This isomer must be formed in its X^2B_2 electronic ground state; recent investigations of a low lying A^2A_1 excited state show that this state is located about 120 kJ mol^{-1} above the ground state, and we expect an exothermicity of only 30 kJ mol^{-1} . Therefore, the majority of the tricarbon hydride products must be formed in the electronic ground state. A minor contribution of $c\text{-}C_3H(A^2A_1)$ cannot be excluded. Finally, we discuss briefly a possible involvement of electronically excited surfaces of cyclopropenylidene. *Ab initio* investigation showed that the first excited 1A_2 and second excited 1B_1 states are energetically accessible lying 241 and 434 kJ mol^{-1} above ground state $c\text{-}C_3H_2$.²⁹ If the reaction

follows C_s symmetry, both electronic wave functions are reduced to an A'' symmetry correlating to the A'' ground state $c\text{-}C_3H$ under C_s symmetry.

Based on these preliminary calculations, electronically excited C_3H_2 intermediates do not play a role in our reaction. It is very interesting to compare our system to the crossed beam reaction of the phenyl radical $C_6H_5(X^2A_1)$, with methylacetylene, $CH_3CCH(X^1A_1)$ at a collision energy of 140 kJ mol^{-1} . This reaction was found to be direct although a bound $(C_6H_5)HCCCH_3$ intermediate exists on the calculated potential energy surface and forms phenylmethylacetylene, $C_6H_5CCCH_3$, and atomic hydrogen. Similar to the $C(^1D)$ plus C_2H_2 collision, the reactant adds to the carbon–carbon triple bond forming a very short lived, highly rovibrationally excited reaction intermediate. The thermodynamically most favorable bicyclic isomer, indene, was not formed in our crossed beam experiment. Most important, microvariational transition state calculations indicate that at very low collision energies the chemical reaction dynamics are completely different from the observed one: indene is the dominating reaction product, and almost no phenylmethylacetylene is formed.³⁰ This is the full consequence of the involved potential energy surface and the enhanced lifetime of the involved intermediate as the initially formed C_9H_9 complex can undergo successive isomerization leading finally to the indene isomer. At higher energy, these calculation correlate fully with our experimental findings, i.e., formation of the phenylmethylacetylene isomer.

We like to point out that Casavecchia *et al.* recently generated a continuous carbon beam via discharge techniques. This beam contains even at very low velocities down to 1000 ms^{-1} electronically excited carbon atoms. Based on our results, we can predict that if the reaction of $C(^1D)$ with C_2H_2 is performed at lower collision energies, the lifetime of the cyclopropenylidene complex should be high enough to allow an energy randomization to occur. Hence, a hydrogen migration to propargylene and/or vinylidenecarbene might be feasible, and three channels to C_3 , $c\text{-}C_3H$, and $l\text{-}C_3H$ may be observable.

VI. COMPARISON WITH THE $C(^3P_j)/C_2H_2$ SYSTEM

The electronic excitation of atomic carbon from the 3P_j to the 1D state has a dramatic effect on the chemical reaction dynamics. As studied at three different collision energies of 8.8–28.0 and 45.0 kJ mol^{-1} , it was found that the reaction involves two microchannels on the triplet surface initiated by addition of $C(^3P_j)$ either to one acetylenic carbon to form trans propenediylidene or to two carbon atoms to yield triplet cyclopropenylidene via loose transition states located at their centrifugal barriers. Triplet propenediylidene rotates around its B/C axis and undergoes [2,3]-H-migration to propargylene, followed by C–H bond cleavage via a symmetric exit transition state to $l\text{-}C_3H(X^2\Pi_j)$ and H. Direct stripping dynamics contribute to the forward-scattered, second microchannel to form $c\text{-}C_3H(X^2B_2)$ and H.

VII. CONCLUSIONS

The reaction between electronically excited carbon atoms, $C(^1D)$, and acetylene was studied at two average collision energies of 45 kJ mol^{-1} and 109 kJ mol^{-1} using the crossed molecular beam technique. The reaction proceeds via direct stripping dynamics on the $^1A'$ surface via an addition of the carbon atom to the π -orbital to form a highly rovibrationally, short lived cyclopropenylidene intermediate which decomposes via atomic hydrogen emission to $c\text{-C}_3\text{H}(X^2B_2)$. The well depth of the rovibrationally excited cyclopropenylidene intermediate along the reaction coordinate is too shallow for an energy randomization to occur. No molecular hydrogen loss channel to tricarbon was observed supporting our experimental findings of an incomplete energy randomization in the initially formed $c\text{-C}_3\text{H}_2$ complex. Based on the involved PES, we can predict the formation of C_3 , $c\text{-C}_3\text{H}$, and $l\text{-C}_3\text{H}$ if this experiment is performed at lower collision energies. Finally, we like to suggest that prospective reaction networks of cometary chemistry must consider distinct product isomers; a simple "guess" and inclusion of the thermodynamically most stable reaction product is not sufficient. The chemical reaction dynamics should be taken into account since the production of thermodynamically unfavorable reaction products is the direct effect of the dynamics and involved potential energy surfaces. The present system is the fourth example studied under single collision conditions which is not governed by its thermochemistry, i.e., $C(^3P_j) + C_6D_6$,³¹ $C_6H_5 + CH_3CCH$,³⁰ and $C_2D + CH_3CCH$.³² The strong energy dependence of the isomer products under extraterrestrial reaction conditions requires incorporation of collision energy and temperature dependent branching ratios to particular isomers in these chemical models.

ACKNOWLEDGMENTS

R.I.K. is indebted the Deutsche Forschungsgemeinschaft for a *Habilitation* fellowship. This work was further supported by Academia Sinica. Thanks to Professor P. Casavecchia (University of Perugia) for comments on this paper. This work was performed within the International Astrophysics Network <http://www.iam.sinica.edu.tw/~kaiser/network.htm>.

- ¹P. Casavecchia, Rep. Prog. Phys. **63**, 355 (2000), and references therein.
- ²P. Casavecchia *et al.*, Acc. Chem. Res. **32**, 503 (1999).
- ³M. Alagia *et al.*, J. Chem. Phys. **108**, 6698 (1998).
- ⁴M. Alagia *et al.*, Chem. Phys. Lett. **258**, 323 (1996).
- ⁵N. Balucani, L. Beneventi, P. Casavecchia, and G. G. Volpi, Chem. Phys. Lett. **180**, 34 (1991).
- ⁶N. Balucani *et al.*, Can. J. Chem. **72**, 888 (1994).
- ⁷M. Alagia, N. Balucani, P. Casavecchia, and G. G. Volpi, J. Phys. A **101**, 6455 (1997).
- ⁸N. Balucani *et al.*, J. Chem. Phys. **94**, 8611 (1991). M. Alagia *et al.*, J. Chem. Soc., Faraday Trans. **91**, 575 (1995).
- ⁹N. Balucani *et al.*, J. Am. Chem. Soc. **122**, 4443 (2000).
- ¹⁰N. Balucani *et al.*, J. Phys. Chem. A **104**, 5655 (2000).
- ¹¹M. Alagia *et al.*, J. Chem. Phys. **110**, 8857 (1999). P. Casavecchia, N. Balucani, and G. G. Volpi, Annu. Rev. Phys. Chem. **50**, 347 (1999).
- ¹²D. C. Scott *et al.*, J. Phys. Chem. **96**, 2509 (1992).
- ¹³A. Bergeat *et al.*, Chem. Phys. Lett. (in press).
- ¹⁴W. F. Huebner, *Physics and Chemistry of Comets* (Springer, Heidelberg, 1990).
- ¹⁵A. D. Becke, J. Chem. Phys. **97**, 9173 (1992).
- ¹⁶C. Lee, W. Yang, and R. G. Parr, Phys. Rev. B **37**, 785 (1988).
- ¹⁷R. Krishnan, M. Frisch, and J. A. Pople, J. Chem. Phys. **72**, 4244 (1988).
- ¹⁸G. D. Purvis and R. J. Bartlett, J. Chem. Phys. **76**, 1910 (1982).
- ¹⁹M. J. Frisch, G. W. Trucks, H. B. Schlegel, P. M. W. Gill, B. G. Johnson, M. A. Robb, J. R. Cheeseman, T. Keith, G. A. Petersson, J. A. Montgomery, K. Raghavachari, M. A. Al-Laham, V. G. Zakrzewski, J. V. Ortiz, J. B. Foresman, J. Cioslowski, B. B. Stefanov, A. Nanayakkara, M. Challacombe, C. Y. Peng, P. Y. Ayala, W. Chen, M. W. Wong, J. L. Andres, E. S. Replogle, R. Gomperts, R. L. Martin, D. J. Fox, J. S. Binkley, D. J. Defrees, J. Baker, J. P. Stewart, M. Head-Gordon, C. Gonzalez and J. A. Pople, GAUSSIAN 94, Revision D.4 (Gaussian, Inc., Pittsburgh, PA, 1995).
- ²⁰MOLPRO is a package of *ab initio* programs written by H.-J. Werner and P. J. Knowles, with contributions from J. Almlöf, R. D. Amos, M. J. O. Deegan, S. T. Elbert, C. Hampel, W. Meyer, K. Peterson, R. Pitzer, A. J. Stone, P. R. Taylor, and R. Lindh.
- ²¹J. F. Stanton, J. Gauss, J. D. Watts, W. J. Lauderdale, and R. J. Bartlett, ACES-II, University of Florida.
- ²²R. I. Kaiser, C. Ochsenfeld, M. Head-Gordon, Y. T. Lee, and A. G. Suits, J. Chem. Phys. **106**, 1729 (1997).
- ²³L. J. Chyall and R. R. Squires, Int. J. Mass. Spectrom. **149/150**, 257 (1995).
- ²⁴R. I. Kaiser, C. Ochsenfeld, M. Head-Gordon, Y. T. Lee, and A. G. Suits, Science **274**, 1508 (1996).
- ²⁵H. Clauberg and P. Chen, J. Am. Chem. Soc. **113**, 1445 (1991).
- ²⁶R. A. Seeburg *et al.*, J. Am. Chem. Soc. **119**, 5847 (1997), and references therein; H. Clauberg, D. W. Minsek, and P. Chen, *ibid.* **114**, 99 (1992).
- ²⁷C. A. Gottlieb *et al.*, J. Chem. Phys. **98**, 4478 (1993).
- ²⁸R. Herges and A. Mebel, J. Am. Chem. Soc. **116**, 8229 (1994).
- ²⁹J. Takahishi and K. Yamashita, J. Chem. Phys. **104**, 6613 (1996).
- ³⁰C. D. Sherrill, C. G. Brandow, W. D. Allen, and H. F. Schaefer III, J. Am. Chem. Soc. **118**, 7158 (1996); A. M. Mebel *et al.*, *ibid.* **120**, 5751 (1998).
- ³¹R. I. Kaiser, O. Asvany, Y. T. Lee, H. F. Bettinger, P. v. R. Schleyer, and H. F. Schaefer III, J. Chem. Phys. **112**, 4994 (2000).
- ³²R. I. Kaiser, I. Hahndorf, L. C. L. Huang, Y. T. Lee, H. F. Bettinger, P. v. R. Schleyer, and H. F. Schaefer III, J. Chem. Phys. **110**, 6091 (1999).
- ³³R. I. Kaiser *et al.*, J. Chem. Phys. (in press).